Elastic Constants of B-A1 Composites by Ultrasonic Velocity Measurements

The elastic stiffness matrix of the composite was determined by direct contact and liquid-immersion through-transmission ultrasonic techniques and is compared to analytical models

by J. H. Gieske and R. E. Allred

ABSTRACT—The complete orthotropic elastic-stiffness matrix of unidirectional, Borsic-filament-reinforced aluminum composites was experimentally evaluated for three different volume fractions by ultrasonic velocity measurements on thin plates. Longitudinal- and shear-velocity measurements were made in appropriate symmetry directions by direct contact or liquid-immersion techniques. The elastic constants determined by this pulsed through-transmission method were in agreement with micromechanical theories based on the properties of the constituent materials. Agreement was also found between engineering constants determined by mechanical testing and those calculated from the ultrasonic data. Finally, measurement of the ultrasonic-wave velocity has also been shown to be a rapid nondestructive-test method for determining filament-volume fraction in a fabricated part.

Introduction and Background

The high specific strength and stiffness of certain fiber-reinforced metals make these materials attractive for use in aerospace applications. However, before these composite systems may be employed in structural applications, the elastic properties must be accurately determined for design purposes. This need is accentuated by the anisotropic material properties which result when high-modulus filaments are incorporated into a low-modulus matrix.

If the reinforcing filaments are unidirectionally aligned in the matrix such that three mutually perpendicular planes of twofold symmetry are produced, the composite is said to be orthotropic and is characterizable by nine independent elastic constants. A composite in which two of the symmetry planes are equivalent exhibits tetragonal symmetry, and elastic deformation may be described by six independent elastic coefficients. A unidirectionally filament-reinforced composite containing a random array of fibers may be considered to be macroscopically isotropic in the plane perpendicular to the fiber direction. The mechanical response of a composite exhibiting such transverse isotropy may be characterized by five independent elastic constants. The assumption of transverse isotropy is often made for convenience in design with unidirectional filament-reinforced composites. The elastic stiffness matrices for composite materials exhibiting orthotropic, tetragonal and transversely isotropic symmetries are the same as those for single crystals and may be found in Ref. 1.

All of the independent elastic constants for anisotropic materials may be determined experimentally by a series of mechanical tests or by ultrasonic-wave-propagation techniques.[1] The ultrasonic technique is more straightforward experimentally and also offers a means of nondestructively measuring the moduli of fabricated structural shapes. This enables comparison of actual values with design objectives in finished parts. The elastic constants resolved ultrasonically are comparable to those determined through mechanical tests, providing the ultrasonic wavelengths used are much larger than the dimensions of the constituent material phases and smaller than the dimensions of the specimen. In this investigation, the ultrasonic-wave-propagation technique has been used to determine the elastic moduli for Borsic-fiber-reinforced aluminum composites.

The complete matrix of independent elastic constants may be found for this case by measuring the ultrasonic wave velocity in the symmetry directions of the composite. The elastic properties of the composite may be evaluated as a function of filament-volume fraction by conducting the experiment on specimens of various fiber contents. The engineering constants such as the Young's moduli, shear moduli and Poisson's ratios may then be determined from the measured independent elastic constants.

Micromechanical theories predicting the elastic constants of fiber-reinforced composites are generally based upon the relative quantities, geometries and elastic properties of the constituent materials. In particular, Behrens[2] has predicted the elastic constants of a filamentary composite having a rectangular fiber array by considering the phase velocity of an ultrasonic wave traveling through the material. Behrens'[2] calculations are based upon the assumptions that the fibers are arranged in rectangular cells which repeat through the lattice and that a theoretically perfect bond exists at the fiber–matrix interface. A perfect bond implies that there is no discontinuity of stresses or displacements across the interface. In this manner, Behrens gives general averaging rules for the nine independent elastic constants for a composite of orthotropic symmetry.

J. H. Gieske and R. E. Allred are associated with Sandia Laboratories, Albuquerque, New Mexico 87115.

Paper was presented under the title "A Nondestructive Measurement of the Elastic Constants of Unidirectional Borsic-fiber-reinforced Aluminum Composites" at Third SESA International Congress on Experimental Mechanics held in Los Angeles, CA on May 13-18, 1973.

Work was supported by the U.S. Atomic Energy Commission.

Original manuscript submitted: March 29, 1973. Final version received: August 10, 1973.

The formulas are not in explicit form for these nine elastic constants; however, if a tetragonal symmetry is present in the composite, the calculations can be simplified by using the Wigner-Seitz approximation, which is a method established in quantum mechanics for the calculation of electron wavefunctions.[3] The Wigner-Seitz approximation assumes that the periodic elemental cell of a composite with two constituents of tetragonal symmetry may be approximated by a circular elemental cell. This allows the introduction of polar coordinates which greatly simplifies the functions of the elastic constants which are complex in Cartesian coordinates. As a result, the elastic constants can be expressed in terms of radial functions alone. Integration of the radial functions is then easily made and the six independent elastic constants for tetragonal symmetry can be written in explicit form as a function of the elastic constants of the two components of the composite and the fiber-volume fraction.

Heaton[4] has also predicted the elastic constants of a unidirectional fiber-reinforced composite of tetragonal symmetry by calculating the microscopic stress and displacement fields which result from constraints on a unit cell subjected to finite strains. The assumption of a perfect bond at the fiber–matrix interface is also necessary for the calculations of Heaton. The two theories agree very well for the range of volume fractions valid in Heaton's calculations, but the explicit expressions given by Behrens are more easily used and cover the entire range of fiber-volume fractions possible. Other authors[5-8] have also proposed theories for the prediction of the elastic properties of composites from the elastic properties of the components; however, their theories include only composites of higher symmetry than tetragonal symmetry, such as ones which are transversely isotropic, hexagonal or having random fiber arrays. Because of the greater utility of the theory of Behrens and its lower symmetry considerations, the values measured in this study will be compared with the theoretical values predicted from Behrens' expressions which are found in Appendix A.

The most highly developed metal-matrix composite system of practical use for structural applications at this time is boron or Borsic*-reinforced aluminum. The B-Al composite system has a high strength and stiffness-to-weight ratio and may be fabricated by conventional plasma-spraying and hot-pressing methods. Because B-Al is being applied to structural applications at the present time, it is appropriate to more fully characterize its deformation behavior by determining the complete matrix of elastic constants for the composite as a function of fiber-volume fraction. The engineering constants of Young's modulus and Poisson's ratio will also be calculated from the elastic constants and compared to recent mechanical-test results.

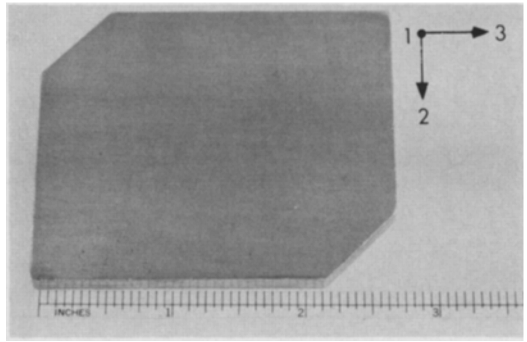

Fig. 1—Specimen of Borsic–aluminum composite plate in the final machined shape

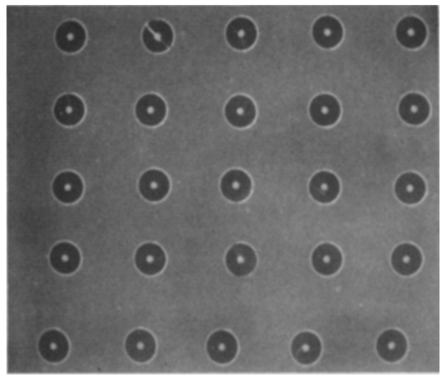

Fig. 2—Photomicrograph showing the 4.2-mil Borsic-fiber distribution for the 0.13-volume-fraction specimen

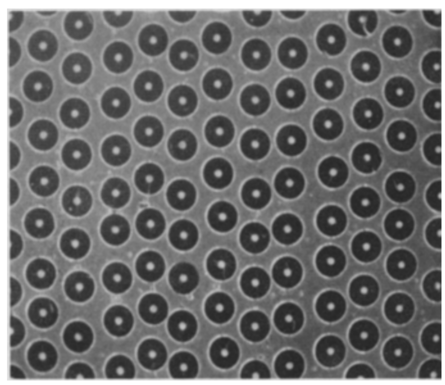

Fig. 3—Photomicrograph showing the 4.2-mil Borsic-fiber distribution for the 0.54-volume-fraction specimen

Description of Material

Composite plates of unidirectional, Borsic-fiber-reinforced aluminum were produced by diffusion bonding plasma-sprayed monolayer tapes at 10 ksi and 555°C for 5 min. Aluminum alloy 1100 was chosen as the matrix and 4.2-mil-diam Borsic fibers as the reinforcement. Details of the fabrication process are given by Hoover, et al.[9] Three plates with different fiber-volume fractions were fabricated for this study. The volume fractions of the plates were altered by varying the fiber spacing and matrix thickness in the monolayer tapes. By chemically analyzing pieces cut

*Borsic is the registered trade name of the silicon carbide coated boron fiber made by Hamilton-Standard Division of United Aircraft Corporation.

from the fabricated plates, the fiber-volume fractions were determined to be 0.13, 0.34 and 0.54. The plates were then machined by grinding with a diamond wheel into rectangles of approximately 2.25 in. by 2.75 in. Corners at a 45-deg angle were then ground off the rectangles which resulted in the specimen shape as shown in Fig. 1. The 45-deg cuts were made in order to measure the ultrasonic-wave velocity on the diagonal of the plate. The thicknesses of the three plates were 0.237, 0.153 and 0.118 in. for the low to high fiber-volume fractions respectively. Photomicrographs of the fiber distribution present in the 13- and 54-volume-percent fiber specimens are shown in Figs. 2 and 3.

Experimental Procedure

Two separate through-transmission methods for measuring the wave velocity in the appropriate symmetry directions of the specimens were used. One technique was the standard ultrasonic pulsed through-transmission method[10] where two opposing transducers of the same frequency are placed in direct contact with two parallel faces of the specimen with a coupling medium (Dow Corning 276-V9 resin). These 0.5-in.-diam transducers were sealed in cases to provide a flat wear plate between the transducer and the specimen face. A zero-time reference mark of the first half-cycle peak of the RF signal was obtained on the oscilloscope by directly coupling two transducers to each other. The specimen was then placed between and coupled to the two transducers with the same coupling medium as before. The time delay of the peak of the first half cycle of the RF signal was then read directly from the oscilloscope. A time-mark generator was used to regularly calibrate the oscilloscope sweep-time base to insure reading the delay time with a maximum error of one percent.

This method was used for longitudinal and shear-wave velocity measurements made in the 1, 2, 3 and 45-deg directions (in the 2-3 plane) which correspond to all parallel faces shown in Fig. 1. The longitudinal velocity values in these directions were measured at frequencies of 2.25, 5 and 10 MHz; in the 1 direction, an additional measurement at 30 MHz was made. The frequency was varied in order to investigate the effect of the thin dimension of the plates on the measured wave velocities. At 10 MHz, the thickness-to-wavelength ratio was as low as 3 in the worst case (i.e., the measurement in the 3 direction of the thinnest plate). Measurements of the wave velocities at 5 and 2.25 MHz which decreased the thickness-to-wavelength ratio by a factor of 4 resulted in only a 3-percent difference between the measured velocities. The use of frequencies higher than 10 MHz was not possible except in the 1 direction because of excessive attenuation of the acoustic wave.

The shear-wave-velocity measurements were not made at frequencies higher than 2.25 MHz, however. This corresponded to a thickness-to-wavelength ratio as low as 1.5 in the worst case. Because the longitudinal wave velocities did not show more than 3-percent change with the thickness-to-wavelength ratio as low as 0.7 at 2.25 MHz, it is assumed that the shear-wave-velocity measurements would be within the same experimental error. In some directions, however, the ultrasonic waveform was distorted and the first half cycle of the wave was not well defined. The difficulty defining the first half cycle of the wave is believed to be the source of some of the 3-percent spread in the measured values. The source of the distortion is unknown but it could have been partially due to the generation of plate waves in addition to volume waves. It is felt that the 3-percent spread in the measured values over the range of frequencies used is not sufficiently serious to invalidate the plane-wave assumption. The plane-wave assumption is thus taken to be valid for this technique in the plate directions, particularly at the 10-MHz frequency.

The second technique which was used to measure the longitudinal and shear velocities in the directions 45 deg to the 1-3 and 45 deg to the 2-3 axes was that described by Markham.[11] The velocity values in these directions must be known in order to calculate the total number of independent elastic constants. The method is an ultrasonic-pulsed through-transmission method with the specimen immersed in a liquid between two opposing transducers which are some distance apart. The method allows one to measure both longitudinal and shear-wave velocities in a wide range of directions on a single specimen without having to cut the specimen normal to these propagating directions.

Figure 4 is a schematic of the experimental apparatus used with the Markham method. Ten-MHz, 3/4-in.-diam well-damped transducers manufactured by Panametrics, Inc., were mounted on opposite sides of a tank. One transducer is used for transmitting the ultrasonic wave in the liquid and the other is used for receiving the wave. The specimen is mounted on a goniometer holder which allows it to be rotated to any given angle relative to the sound beam and the angle can then be read from the gonimeter. With the specimen in place with its sides perpendicular to the longitudinal-wave sound beam in the liquid, a difference in the delay time for the ultrasonic wave to travel between the two transducers will be observed and compared to the delay time for the ultra-

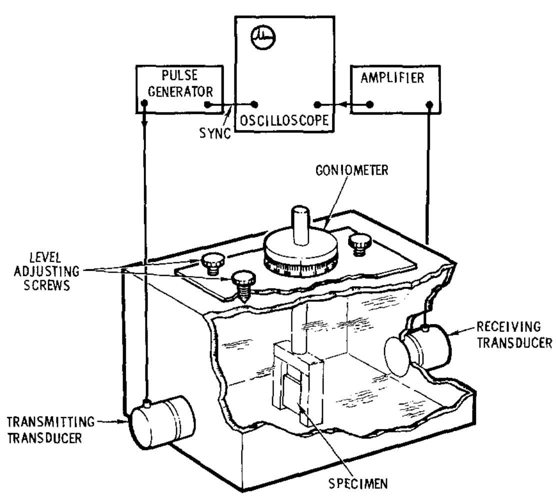

Fig. 4—Schematic of liquid-immersion through-transmission technique for measuring ultrasonic longitudinal and shear-wave velocities in off-normal directions of a thin specimen

sonic wave to travel between the transducers with no specimen in the sound path. By using the difference in delay time observed on an oscilloscope, the longitudinal velocity, V_L, in the specimen is given by

$$V_L = \frac{1}{1/V_{liq} + \Delta t/d} \tag{1}$$

where V_{liq} is the longitudinal-wave velocity in the liquid, d is the specimen thickness and Δt is the observed difference in delay time caused by the specimen being inserted in the sound-beam path.

For the specimen inclined at an angle to the ultrasonic path, the longitudinal wave at the specimen–liquid interface splits into a longitudinal wave and a shear wave in the specimen as shown by Fig. 5. The longitudinal wave refracts at an angle given by

$$\frac{V_L}{V_{liq}} = \frac{\sin r}{\sin i} \tag{2}$$

where r is the refracted angle for the incident angle i and V_L is the longitudinal-wave velocity in the direction r. The shear wave generated in the specimen at the liquid–specimen interface propagates in a different direction r' which is given by a similar expression

$$\frac{V_S}{V_{liq}} = \frac{\sin r'}{\sin i} \tag{3}$$

where V_S is the shear-wave velocity in the specimen in the direction r' for the incident angle i. The shear-wave mode again converts to a longitudinal wave at the second specimen–liquid interface and a characteristic delay time for this case is observed on the oscilloscope.

The difference in delay time for the longitudinal wave with and without the specimen in place at an angle i is given by

$$\Delta t = \frac{d}{V_L \cos r} - d\left(\frac{\cos i + \sin i \tan r}{V_{liq}}\right) \tag{4}$$

from which the refraction angle r is given by

$$r = \tan^{-1}\left(\frac{\sin i}{\Delta t\, V_{liq}/d + \cos i}\right) \tag{5}$$

Similar expressions are true for the shear wave where V_L and r are replaced by V_S and r'. Therefore by measuring i and Δt for the longitudinal and shear waves, one can calculate r and r' from eq (5) and then V_L and V_S from eqs (2) and (3). It should be noted that the use of eqs (2) and (3) with eqs (4) and (5) assumes that the energy beam of the ultrasonic wave travels in the same direction as the wave normal. The two do not, in general, coincide in anisotropic media.[12] Although the delay times of the two are equal for wave propagation between parallel specimen faces which are perpendicular to the wave normal, the path length of the energy beam is larger since it is at an angle to the wave normal. Hence, the velocity associated with the energy beam is faster and is designated the group velocity of the sound waves. The sound-wave velocity in the direction of the wave normal is the phase velocity. The delay time measured by the liquid-immersion technique is that of the group velocity through the specimen. The distance the wave travels through the specimen, however, is calculated as if it were the phase velocity. Since the specimen is tilted at an angle, the actual path of the energy beam can be longer or shorter than that calculated by eq (4) depending upon the angle between the wave normal and the energy-beam direction.

To obtain the longitudinal-wave velocity and the shear-wave velocity at 45 deg with respect to the specimen faces, the time-delay difference for the two waves was measured over a large range of incident angles which gave refracted longitudinal and shear waves below and above the 45-deg directions. By calculating the refracted angles and corresponding

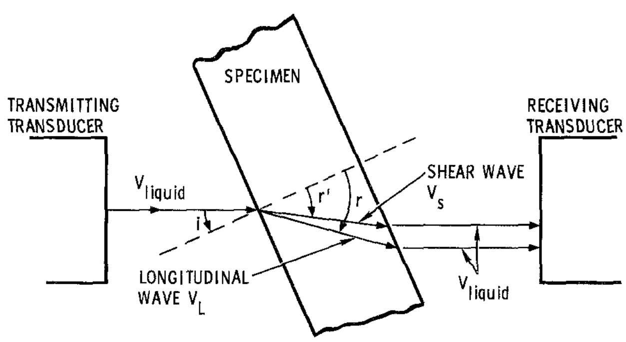

Fig. 5—Refracted-longitudinal and mode-converted shear-wave propagation in the specimen and liquid between the ultrasonic transducers

TABLE 1—MEASURED LONGITUDINAL AND SHEAR VELOCITIES IN IN./μS. IN THE 1-2 AND 1-3 PLANES FOR BORSIC-FIBER-REINFORCED ALUMINUM COMPOSITES

		Fiber-volume Fraction					
		.13		.34		.54	
1-2 Plane		Long.	Shear	Long.	Shear	Long.	Shear
1	0°	.269	.132	.298	.151	.338	.170
	30	.270	.132	.297	.150	.335	.175
	35	.270	.133	.298	.150	.335	.178
	40	.270	.133	.296	.151	.335	.182
	45	.270	.134	.295	.153	.335	.185
	50	.270	.134	.296	.153	.333	.185
	55	.270	.134	.296	.153	.331	.185
	60	.270	.133	.296	.153	.331	.183
	65	.270	.133	.294	.151	.329	.178
	70	.270	.132	.290	.149	.327	.173
2	90	.268	.135	.287	.147	.312	.171
1-3 Plane							
1	0°	.269	.135	.298	.159	.338	.187
	30	.272	.144	.299	.178	.348	.217
	35	.274	.146	.302	.182	.350	.217
	40	.275	.149	.305	.183	.354	.219
	45	.277	.150	.309	.183	.360	.221
	50	.280	.148	.316	.179	.365	.218
	55	.282	.144	.318	.175	.375	.213
	60	.284	.142	.320	.172	.378	.207
	65	.286	.140	.322	.167	.381	.194
	70	.288	.138	.323	.164	.382	.193
3	90	.296	.143	.350	.161	.393	.189

velocity values for a wide range of incident angles, the velocity value at 45 deg could be ascertained easily.

Results and Discussion

The longitudinal- and shear-wave-velocity values obtained in the 1-2 and 1-3 planes are shown in Table 1. The values at 0 and 90 deg were determined by the direct-contact through-transmission technique. All other values reported in Table 1 were determined by the liquid-immersion through-transmission technique. The balance of the longitudinal and shear velocities measured by the direct-contact through-transmission method is listed in Table 2.

The data show that the longitudinal- and shear-wave velocities are isotropic in the 13-volume-percent fiber specimen in the 1-2 plane. The longitudinal- and shear-wave velocities in the 1-2 plane for the 54-volume-percent fiber specimen do not show this isotropy however, which indicates that this specimen is more orthotropic. Examination of the fiber distributions in Figs. 2 and 3 shows that this is an expected result. The assumption of tetragonal symmetry is certainly justified from the square array of fiber spacing in the 0.13-volume-fraction specimen; however, in the higher volume-fraction specimen (0.54), it appears that the composite becomes more orthotropic in its symmetry, i.e., the fiber spacings in the 1 and 2 directions are not equal. The values of the longitudinal- and shear-velocities given in Table 1 for the 45-deg direction in the 1-2 and 1-3 planes are used in the expressions for the calculation of the elastic constants. Table 2 shows these values along with all the other longitudinal and shear velocities measured in the appropriate symmetry directions for calculation of all the elastic constants. Table 2 lists the directions of propagation, the velocity mode, the velocity values, and the velocity designation for the calculation of the elastic constants for the three specimens.

Table 3 lists the elastic constants which were calculated from the velocities listed in Table 2. The elastic constants are defined in the Voigt notation[1] with the 3 axis taken in the direction of the Borsic fibers and the 1 axis taken in the thickness direction of the plates. The elastic constants are defined with the assumption, which is assumed valid in this case, that only plane-wave propagation of the sound waves is present. C_{12}, C_{13} and C_{23} are taken to be positive since only the absolute value can be determined by the calculations. The positive values are consistent with the material-stability conditions[13] and the subsequent agreement between the Young's modulus and Poisson's ratio as calculated from the elastic constants and those determined experimentally by mechanical tests.

The elastic constants listed in Table 3 also reveal that the higher fiber-volume-fraction specimens are somewhat orthotropic since $C_{11} \neq C_{22}$ and C_{12}, C_{13} and C_{23} are not equal. The values of C_{12}, C_{13} and C_{23} calculated from the longitudinal-wave velocity deviate from the same values calculated from the shear-wave velocity at the higher volume fractions. The magnitudes of these constants are very sensitive to the velocity values, however, and a change of either the longitudinal or shear velocity by 2 percent brings

TABLE 2—MEASURED ULTRASONIC-VELOCITY VALUES FOR THE THREE FIBER-VOLUME-FRACTION SPECIMENS OF BORSIC-ALUMINUM COMPOSITES IN ALL OF THE APPROPRIATE SYMMETRY DIRECTIONS FOR CALCULATION OF THE ELASTIC CONSTANTS OF ORTHOTROPIC SYMMETRY

Values are in in./μs

Propagation Direction[a]	Velocity Mode[b]	Fiber-volume Fraction .13	.34	.54	Velocity Designation
1	L	.269	.298	.338	V_1
	Tpol 2	.132	.151	.170	V_3
	Tpol 3	.135	.159	.187	V_2
2	L	.268	.287	.312	V_7
	Tpol 1	.135	.147	.171	V_9
	Tpol 3	.135	.154	.182	V_8
3	L	.296	.350	.393	V_{13}
	Tpol 1	.143	.161	.189	V_{15}
	Tpol 2	.143	.163	.194	V_{14}
45 1,2	L	.270	.295	.335	V_{16}
	Tpol $\overline{1}$,2	.134	.153	.185	V_{18}
45 1,3	L	.277	.309	.360	V_{10}
	Tpol $\overline{1}$, 3	.150	.183	.221	V_{12}
45 2,3	L	.276	.309	.338	V_4
	Tpol $\overline{2}$,3	.148	.173	.204	V_6
	Tpol 1	.136	.154	.187	V_5

[a] 45 2,3 means the plane cut at 45 deg to the 2,3 axes and parallel to the 1 axis. $\overline{1}$ means minus 1 direction.
[b] L means longitudinal, Tpol 3 means transverse with direction of polarization in the 3 direction.

TABLE 3—ELASTIC STIFFNESS FOR BORSIC–ALUMINUM COMPOSITES CALCULATED FROM VELOCITY VALUES GIVEN IN TABLE 2

Values are in units of 10^6 psi. The density for each fiber-volume-fraction specimen is given in gm/cc

	Fiber-volume Fraction .13, $\rho = 2.69$	.34, $\rho = 2.65$	.54, $\rho = 2.65$
$C_{11} = \rho V_1^2$	18.21	22.02	28.32
$C_{55} = \rho V_2^2$	4.57	6.27	8.67
$C_{66} = \rho V_3^2$	4.39	5.65	7.17
$C_{22} = \rho V_7^2$	18.07	20.42	24.13
$C_{44} = \rho V_8^2$	4.59	5.88	8.21
$C_{66} = \rho V_9^2$	5.29	5.36	7.25
$C_{33} = \rho V^2_{13}$	22.05	30.37	38.29
$C_{44} = \rho V^2_{14}$	5.15	6.59	9.33
$C_{55} = \rho V^2_{15}$	5.15	6.43	8.86
$\frac{1}{2}(C_{55} + C_{66}) = \rho V_5^2$	4.66	5.88	8.67
$\lvert C_{12}\rvert$ V_{16}[a]	8.87	10.90	14.90
$\lvert C_{12}\rvert$ V_{18}[a]	9.11	9.59	9.12
$\lvert C_{13}\rvert$ V_{10}[b]	8.62	7.85	12.86
$\lvert C_{13}\rvert$ V_{12}[b]	8.67	9.03	8.38
$\lvert C_{23}\rvert$ V_4[c]	8.39	8.67	6.31
$\lvert C_{23}\rvert$ V_6[c]	8.89	9.80	9.24

[a] $|C_{12}| = \frac{1}{2}\{[4\rho V^2 - (C_{11} + C_{22} + 2C_{66})]^2 - (C_{11} - C_{22})^2\}^{1/2} - C_{66}$ where V is the designated velocity above.
[b] Same formula as (a) except index changes $2\rightarrow3$, and $6\rightarrow5$.
[c] Same formula as (a) except index changes $1\rightarrow2$, $2\rightarrow3$, and $6\rightarrow4$.

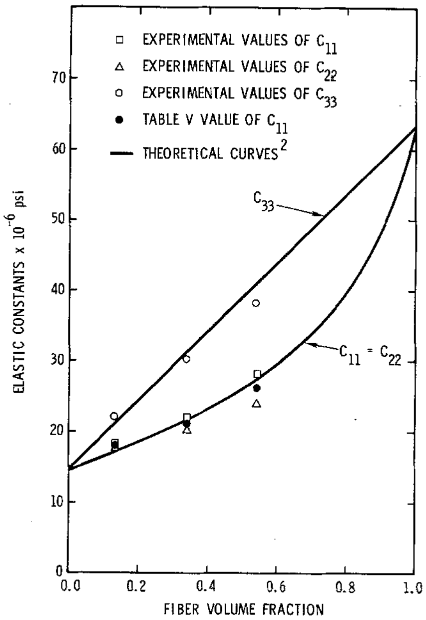

Fig. 6—Theoretical and experimental elastic constants C_{11}, C_{22} and C_{33} vs. fiber-volume fraction for tetragonal symmetry

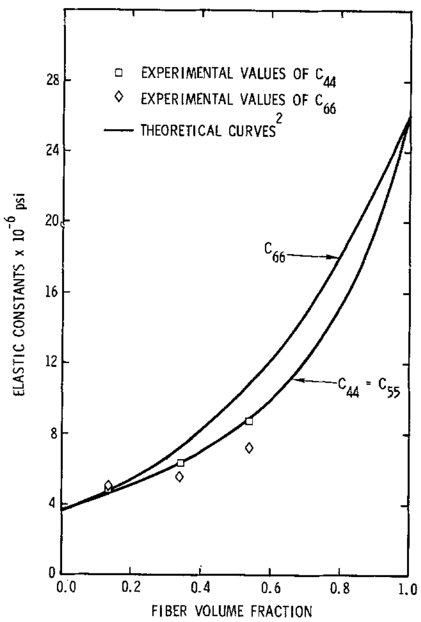

Fig. 7—Theoretical and experimental elastic constants C_{44} and C_{66} vs. fiber-volume fraction for tetragonal symmetry

the two calculated values into agreement. For this reason, the uncertainties in these quantities might be as much as 50 percent whereas the uncertainty in the other elastic constants is approximately 7 percent. Since C_{44}, C_{55} and C_{66} are found by more than one velocity measurement, the average values were used in the formulas for the calculations of C_{12}, C_{13} and C_{23}.

The nine orthotropic elastic stiffnesses and compliances calculated from the ultrasonic-velocity data

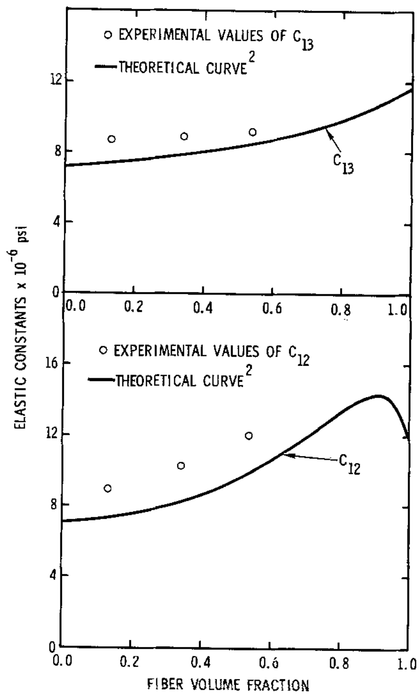

Fig. 8—Theoretical and experimental elastic constants C_{12} and C_{13} vs. fiber-volume fraction for tetragonal symmetry

for each fiber-volume fraction are given in Table 4. Average values of all equal constants listed in Table 3 were used in calculating the values presented in Table 4. Examination of C_{11} and C_{22} in Table 4 indicates that the assumption of transverse isotropy

TABLE 4—ELASTIC STIFFNESSES AND COMPLIANCES FOR BORSIC-ALUMINUM COMPOSITES OF ORTHOTROPIC SYMMETRY

Stiffnesses are in units of 10^6 psi and compliances are in units of 10^{-8} psi^{-1}

Constants	Values per Fiber-volume Fraction .13	.34	.54
C_{11}	18.21	22.02	28.32
C_{12}	8.99	10.25	12.01
C_{13}	8.65	8.44	10.62
C_{22}	18.07	20.42	24.13
C_{23}	8.64	9.24	7.77
C_{33}	22.05	30.37	38.29
C_{44}	4.87	6.23	8.77
C_{55}	4.87	6.35	8.76
C_{66}	4.84	5.51	7.21
S_{11}	7.886	6.126	4.746
S_{12}	−3.008	−2.673	−2.074
S_{13}	−1.915	−0.889	−0.896
S_{22}	7.957	6.845	5.340
S_{23}	−1.938	−1.340	−0.508
S_{33}	6.046	3.948	2.963
S_{44}	20.534	16.051	11.403
S_{55}	20.534	15.748	11.416
S_{66}	20.661	18.149	13.870

results in an error of about 15 percent for the 0.54-volume-fraction specimens. The assumption of transverse isotropy in the case of the off-diagonal constants C_{13} and C_{23} results in an error of 25 percent. It may be seen that the assumption of transverse isotropy in the case of high-volume-fraction composites may introduce an error greater than the design allowable, in which case the complete orthotropic matrix of elastic constants should be used.

For comparison with the theory given by Behrens,[2] a tetragonal symmetry must be assumed for all the specimens. The six independent elastic constants for the composite displaying tetragonal symmetry are given for each fiber-volume fraction in Table 5. Constants listed in Table 4 which are equivalent assuming tetragonal symmetry were averaged for presentation in Table 5.

The elastic stiffnesses listed in Table 5 are plotted in Figs. 6, 7 and 8 as a function of fiber-volume fraction. The predicted dependence of the elastic constants on fiber-volume fraction as calculated from the expressions in Appendix A is also shown in Figs. 6, 7 and 8. The material properties used in these expressions for the Borsic fibers and aluminum matrix are given in Table 6. Good agreement exists between the experimental and theoretical values for the constants C_{11}, C_{33} and C_{44}. Agreement is not as good for the constants C_{12} and C_{13}; however, these quantities are very sensitive to errors in the ultrasonic-wave-velocity measurements. The constant C_{66} shows the maximum deviation from theory as calculated from eq (A4) in Appendix A for the higher filament-volume fractions. This indicates that shear coupling between the fibers and matrix may not be as strong as that considered in theory due to the manufacturing process, i.e., a theoretically perfect bond does not exist at the fiber–matrix interface.

Young's moduli, shear moduli and Poisson's ratios were calculated from the data in Table 5 for composites of tetragonal symmetry for each volume fraction and are listed in Table 7. Expressions for these engineering constants in terms of the elastic constants for orthotropic symmetry are given in Appendix B. Also listed in Table 7 are the values of E_{33} and ν_{31} which were experimentally determined for Borsic–aluminum by mechanical testing.[14] Agreement is found to within 6 percent between the mechanically measured values of Young's moduli, E_{33}, and Poisson's ratio, ν_{31}, and the values calculated from the ultrasonic data. This agreement, in addition to the agreement between theoretically predicted values and the values resolved in this study, indicates that the ultrasonic-wave-propagation technique is a valid method for determining the elastic properties of fiber-reinforced composites. This agreement also indicates that the composite may be considered a quasi-homogeneous medium for the theoretical prediction of elastic constants.

The theoretical curve for C_{33} was obtained by using the upper limit of Young's modulus for the Borsic fibers. Actually, Young's modulus for a single Borsic fiber is between 55 and 60-million psi.[15] From a straight-line extrapolation of the experimental points (Fig. 6), it appears that the average Young's modulus for the Borsic fibers is closer to 55-million psi.

Since the ultrasonic velocity in the fiber direction is proportional to the filament content as seen in Fig. 6, this method provides a quick nondestructive means of measuring the filament-volume fraction of a part whose geometry prohibits such a determination. The ultrasonic velocity measurements also provide a check on the moduli in the principal directions which can be

TABLE 5—ELASTIC STIFFNESSES AND COMPLIANCES FOR BORSIC–ALUMINUM COMPOSITES OF TETRAGONAL SYMMETRY

Stiffnesses are in units of 10^6 psi and compliances are in units of 10^{-8} psi^{-1}

	Values per Fiber-volume Fraction		
Constants	.13	.34	.54
C_{11}	18.14	21.22	26.23
C_{12}	8.99	10.25	12.01
C_{13}	8.64	8.84	9.20
C_{33}	22.05	30.37	38.29
C_{44}	4.87	6.29	8.77
C_{66}	4.84	5.51	7.21
S_{11}	7.920	6.457	4.995
S_{12}	−3.001	−2.658	−2.038
S_{13}	−1.925	−1.106	−0.710
S_{33}	6.043	3.936	2.953
S_{44}	20.534	15.898	11.403
S_{66}	20.661	18.149	13.870

TABLE 6—ELASTIC PROPERTIES OF BORSIC FIBER AND 1100 ALUMINUM MATRIX

	Borsic	Aluminum
Young's Modulus	55-60 $\times 10^6$ psi[15]	10 $\times 10^6$ psi
Poisson's Ratio[14]	.156	.327
Density	2.69 g/cc	2.70 g/cc
C_{11}	63.67 $\times 10^6$ psi	14.66 $\times 10^6$ psi
$C_{12} = \lambda_1$	11.77 $\times 10^6$ psi	7.12 $\times 10^6$ psi
$C_{44} = \mu_1$	25.95 $\times 10^6$ psi	3.77 $\times 10^6$ psi

TABLE 7—YOUNG'S MODULI (E_{ii}), POISSON'S RATIOS (ν_{ij}), AND SHEAR MODULI (G_{ij}) FOR BORSIC–ALUMINUM COMPOSITES OF TETRAGONAL SYMMETRY

Moduli are in units of 10^6 psi

	Values per Fiber-volume Fraction		
	.13	.34	.54
E_{11}	12.65	15.51	20.02
E_{33}	16.52	25.42	33.87
ν_{12}	.38	.41	.41
ν_{13}	.24	.17	.14
ν_{31}	.32	.28	.24
G_{23}	4.87	6.29	8.77
G_{12}	4.84	5.51	7.21
E_{33}≠	15.3	24.3	31.5
ν_{31}≠	.30	.27	.22

≠Young's modulus and Poisson's ratio determined from mechanical tests.[11]

compared to the required moduli for which the fabricated part was designed.

Summary and Conclusions

The complete orthotropic matrix of nine independent elastic constants for Borsic–aluminum composites has been determined for each of three fiber-volume fractions by ultrasonic-wave-propagation techniques. These values may be used in design with Borsic–aluminum composites rather than assuming a higher symmetry condition, such as transverse isotropy. The assumption of transverse isotropy has been shown to be 15 to 25 percent in error for the specimens measured in this study.

The orthotropic data have been reduced to matrices of six independent elastic constants by assuming that tetragonal symmetry exists in the composite. These results are compared with theoretical predictions for the elastic constants of composites exhibiting tetragonal symmetry and are in good agreement for the coefficients C_{11}, C_{33} and C_{44}. The experimental values of C_{12} and C_{13} show a larger deviation from theory but are very sensitive to experimental errors. The constant C_{66} shows the largest deviation from theory which indicates that the fiber-matrix interface in the composite is not a theoretically perfect bond.

The engineering constants Young's modulus and Poisson's ratio were also calculated from the elastic constants of the composite assuming tetragonal symmetry. Agreement was found to be within 6 percent between these values and those determined from mechanical tests. The agreement between the values determined in this study and values predicted by theory and resolved by mechanical testing indicates that the ultrasonic-wave-propagation technique is a valid method for determining the elastic properties of filament-reinforced composites. Measurement of the ultrasonic-wave velocity has also been shown to be a rapid nondestructive-test method for determining filament-volume fraction in a fabricated part.

References

1. *Huntington, H. B., "The Elastic Constants of Crystals," Solid State Physics, **7**, Academic Press, New York, 213-351 (1958).*
2. *Behrens, E., "Elastic Constants of Filamentary Composites with Rectangular Symmetry," J. Acoust. Soc. Amer., **42**, 367 (1967).*
3. *Kittel, C., Quantum Theory of Solids, John Wiley and Sons, New York, 250-254 (1963).*
4. *Heaton, M. D., "A Calculation of the Elastic Constants of a Unidirectional Fibre-Reinforced Composite," Brit. J. Appl. Phys. (J. Phys. D.), **1**, 1039 (1968).*
5. *Whitney, J. M. and Riley, M. B., "Elastic Properties of Fiber-Reinforced Composite Materials," AIAA J., **4**, 1537 (1966).*
6. *Hashin, Z. and Rosen, B. W., "The Elastic Moduli of Fiber-Reinforced Materials," J. Appl. Mech., **31**, 223 (1964).*
7. *Davies, W. E. A., "The Elastic Constants of a Two-Phase Composite Material," J. Phys. D.: Appl. Phys., **4**, 1176 (1971).*
8. *Greszczuk, L. B., "Theoretical and Experimental Studies on Properties and Behavior of Filamentary Composites," Douglas Paper No. 3550, MDAC-WD, Santa Monica, CA (1966).*
9. *Hoover, W. R., Allred, R. E., Moss, M. and Cyrus, W. L., "Metal-Matrix Composite Fabrication by Plasma Spraying and Tape Bonding," Sandia Laboratories Report SC-TM-710396 (July 1971).*
10. *Zimmer, J. E. and Cost, J. R., "Determination of the Elastic Constants of a Unidirectional Fiber Composite Using Ultrasonic Velocity Measurements," J. Acoust. Soc. Amer., **47**, 795 (1970).*
11. *Markham, M. F., "Measurement of the Elastic Constants of Fibre-Composites by Ultrasonics," Composites, **1**, 145 (1970).*
12. *Henneke II, E. G., "Reflection-Refraction of a Stress Wave at a Plane Boundary between Anisotropic Media," J. Acoust. Soc. Amer., **51**, 210 (1972).*
13. *Alers, G. A. and Neighbours, J. R., "Crystal Stability and Elastic Constants," J. Appl. Phys., **28**, 1514 (1957).*
14. *Allred, R. E., "Elastic-Plastic Poisson's Ratio of Borsic-Reinforced Aluminum Composites," Sandia Laboratories Rept. SC-RR-720924 (Dec. 1972).*
15. *Herring, H. W., "Selected Mechanical and Physical Properties of Boron Filaments," NASA-TND-3202, NASA, Langley Research Center (1966).*

APPENDIX A

The six independent elastic constants for a two-component composite with tetragonal symmetry as given by Behrens[2] as a function of fiber-volume content are given below. The Lamé coefficients λ and μ are used where 1 and 2 designate the fiber coefficients and matrix coefficients respectively. S is the fiber-volume fraction and q equals $(2\mu_2 + \lambda_2)/\mu_2$.

$$C_{11} = C_{22} = (2\mu_2 + \lambda_2) \left[\frac{\mu_1 + \lambda_1 + \mu_2}{(\mu_1 + \lambda_1 + \mu_2) - (\mu_1 + \lambda_1 - \mu_2 - \lambda_2)S} + \frac{(\mu_1 - \mu_2)S}{(\mu_1 + \mu_2 + \lambda_2) - (\mu_1 - \mu_2)S^q} \right] \quad \text{(A1)}$$

$$C_{33} = (2\mu_2 + \lambda_2) + (2\mu_1 + \lambda_1 - 2\mu_2 - \lambda_2)S - \frac{(\lambda_1 - \lambda_2)^2\, S(1 - S)}{(\mu_1 + \lambda_1 + \mu_2) - (\mu_1 + \lambda_1 - \mu_2 - \lambda_2)S} \quad \text{(A2)}$$

$$C_{44} = C_{55} = \mu_2 \frac{(\mu_1 + \mu_2) + (\mu_1 - \mu_2)S}{(\mu_1 + \mu_2) - (\mu_1 - \mu_2)S} \quad \text{(A3)}$$

$$C_{66} = \mu_2 \left[1 + \frac{(\mu_1 - \mu_2)S}{\mu_1 - (\mu_1 - \mu_2)S^{1/q}} \right] \quad \text{(A4)}$$

$$C_{12} = \lambda_2 + (2\mu_2 + \lambda_2)\, S \left[\frac{\mu_1 + \lambda_1 - \mu_2 - \lambda_2}{(\mu_1 + \lambda_1 + \mu_2) - (\mu_1 + \lambda_1 - \mu_2 - \lambda_2)S} - \frac{\mu_1 - \mu_2}{(\mu_1 + \mu_2 + \lambda_2) - (\mu_1 - \mu_2)S^q} \right] \quad \text{A(5)}$$

$$C_{13} = C_{23} = \lambda_2 + \frac{(\lambda_1 - \lambda_2)(2\mu_2 + \lambda_2)S}{(\mu_1 + \lambda_1 + \mu_2) - (\mu_1 + \lambda_1 - \mu_2 - \lambda_2)S} \quad \text{(A6)}$$

APPENDIX B

The following expressions are used for calculating Young's moduli, Poisson's ratios, and shear moduli from the elastic constants for tetragonal symmetry.

$$E_{11} = C_{11} - \nu_{13} C_{13} - \nu_{12} C_{12} \quad \text{(B1)}$$

$$E_{33} = C_{33} - 2\nu_{31} C_{13} \quad \text{(B2)}$$

$$\nu_{12} = \frac{C_{13}^2 - C_{12} C_{33}}{C_{13}^2 - C_{11} C_{33}} \quad \text{(B3)}$$

$$\nu_{13} = \frac{C_{12} C_{13} - C_{11} C_{13}}{C_{13}^2 - C_{11} C_{33}} \quad \text{(B4)}$$

$$\nu_{31} = \frac{C_{12} C_{13} - C_{11} C_{13}}{C_{12}^2 - C_{11}^2} \quad \text{(B5)}$$

$$G_{23} = C_{44} \quad \text{(B6)}$$

$$G_{12} = C_{66} \quad \text{(B7)}$$